Proc. Natl. Acad. Sci. USA
Vol. 90, pp. 9436–9440, October 1993
Pharmacology

Molecular dissection of subunit interfaces in the acetylcholine receptor: Identification of residues that determine curare selectivity

STEVEN M. SINE

Department of Physiology and Biophysics, Mayo Clinic, 200 First Street SW, Rochester, MN 55905

Communicated by Clay M. Armstrong, June 21, 1993 (received for review April 13, 1993)

ABSTRACT **The acetylcholine receptor from vertebrate skeletal muscle is a transmembrane channel that binds nerve-released acetylcholine to elicit rapid transport of small cations. Composed of two α subunits and one β, one γ, and one δ subunit, the receptor is a cooperative protein containing two sites that bind agonists, curariform antagonists, and snake α-toxins. Until recently the two binding sites were thought to reside entirely within each of the two α subunits, but affinity labeling and expression studies have demonstrated contributions by the γ and δ subunits. Affinity labeling and mutagenesis studies have identified residues of the α subunit that contribute to the binding site, but the corresponding γ- and δ-subunit residues remain unknown. By making γ–δ chimeras and following the nearly 100-fold difference in curare affinity for the two binding sites, the present work identified residues of the γ and δ subunits likely to be near the binding site. Two sets of binding determinants were identified in homologous positions of the γ and δ subunits. The determinants lie on either side of a disulfide loop found within the major extracellular domain of the subunits. This loop is common to all acetylcholine, γ-aminobutyrate, and glycine receptor subunits.**

In the native acetylcholine receptor (AChR), the two ligand binding sites show very different affinities for both acetylcholine (1) and curariform antagonists (2, 3). Because acetylcholine must occupy both sites to open the channel, the high-affinity site allows priming of the AChR for rapid activation, whereas the low-affinity site causes the AChR to shut off abruptly following a stimulus (4). For curare, the affinity difference means that it blocks activation by binding to only the high-affinity site (3). The molecular basis for the different affinities is thought to reside within the portions of the γ and δ subunits that contact the two α subunits to form the binding sites.

Recent work showed that AChRs lacking either a γ or a δ subunit assemble into pentamers with subunit compositions, $\alpha_2\beta\gamma_2$ and $\alpha_2\beta\delta_2$ (5). More symmetrical than native $\alpha_2\beta\gamma\delta$ AChRs, these triplet AChRs bind curare with a single affinity—high affinity for $\alpha_2\beta\gamma_2$ and low affinity for $\alpha_2\beta\delta_2$—to quantitatively account for the two affinities seen in the native AChR. Thus, studies of triplet AChRs, as well as studies of $\alpha\gamma$ and $\alpha\delta$ subunit pairs (6), demonstrate that the γ subunit confers high affinity for curare, whereas the δ subunit confers low affinity. In the work described here, determinants responsible for the different curare affinities were identified by constructing δ–γ subunit chimeras, coexpressing them with α and β subunits, and measuring binding of the curariform antagonist (+)-dimethyltubocurarine (DMT).

METHODS

Construction of Chimeras and Point Mutations. Mouse AChR cDNAs (7, 8) were subcloned into a cytomegalovirus-based expression vector (9). Mutations were introduced either by ligating DNA fragments at common restriction sites, or by identifying restriction sites on either side of the desired mutation, and bridging the two sites with synthetic double-stranded oligonucleotides. Chimeras are designated as follows: the first letter gives the subunit from which N-terminal sequence is taken, G for γ and D for δ; the following number gives the position of the chimeric junction, using the δ subunit as reference, and the final letter gives the subunit for C-terminal sequences. All constructs were confirmed by restriction mapping and dideoxy sequencing. Chimeras and mutant subunits were constructed as follows.

D225G. Delta-pRBG4 was digested with *Ear* I to yield an 1800-bp fragment, which was treated with mung bean nuclease followed by *Xba* I to yield a 760-bp δ fragment. Gamma-pRBG4 was digested with *Ava* I to yield an 1193-bp fragment, which was digested with *Ear* I to yield a 407-bp γ fragment. After treatment with the Klenow fragment of DNA polymerase I in the presence of the four dNTPs, the 407-bp γ fragment was digested with *Alw*NI to yield the 362-bp γ fragment. Gamma-pRBG4 was digested with *Xba* I and *Alw*NI, and the resulting 2820- and 1580-bp fragments were religated and digested with *Xba* I to yield the 4400-bp *Alw*NI–*Xba* I γ fragment. The 760-bp δ, 407-bp γ, and 4400-bp γ fragments were ligated to yield D225G.

G100D225G. Gamma-pRBG4 was digested with *Spe* I and then *Bst*EII to yield a 3900-bp γ fragment. Gamma-pRBG4 was digested with *Tth*111I and *Spe* I to yield a 1050-bp γ fragment. D225G was digested with *Spe* I and *Bst*EII to yield a 1700-bp fragment, which was digested with *Bpm* I to yield the 590-bp δ–γ *Bpm* I–*Bst*EII fragment. The 3900-bp *Bst*EII–*Spe* I γ, 1050-bp *Spe* I–*Tth*111I γ, and 590-bp *Bpm* I–*Bst*EII δ–γ fragments were ligated in the presence of the trinucleotide GCT to yield G100D225G.

G175D225G. Gamma-pRBG4 and D225G were digested with *Spe* I and *Pfl*MI and the respective 1280- and 4260-bp fragments were isolated. The 4260-bp *Pfl*MI–*Spe* I δ–γ fragment was ligated with the 1280-bp *Spe* I–*Pfl*MI γ fragment to yield G175D225G.

G131D225G. D225G was digested with *Xba* I and *Pfl*MI to yield a 4850-bp *Pfl*MI–*Xba* I δ–γ fragment. Gamma-pRBG4 was digested with *Xba* I and *Pfl*MI to yield a 660-bp fragment, which was digested with *Hph* I to yield a 541-bp *Xba* I–*Hph* I γ fragment. Delta-pRBG4 was digested with *Pfl*MI to yield a 356-bp fragment, which was digested with *Hph* I to yield a 130-bp *Hph* I–*Pfl*MI δ fragment. The 4850-bp *Pfl*MI–*Xba* I δ–γ, 541-bp *Xba* I–*Hph* I γ, and 130-bp *Hph* I–*Pfl*MI δ fragments were ligated to yield G131D225G.

G131D156G. Gamma-pRBG4 was digested with *Xba* I and *Bst*XI to yield a 4936-bp *Bst*XI–*Xba* I γ fragment. G131D225G was digested with *Xba* I and *Kpn* I to yield an 800-bp fragment, which was digested with *Sty* I to yield a

The publication costs of this article were defrayed in part by page charge payment. This article must therefore be hereby marked "*advertisement*" in accordance with 18 U.S.C. §1734 solely to indicate this fact.

Abbreviations: AChR, acetylcholine receptor; DMT, (+)-dimethyltubocurarine.

560-bp *Xba* I–*Sty* I γ–δ fragment. The 4936-bp *Bst*XI–*Xba* I γ and 560-bp *Xba* I to *Sty* I γ–δ fragments were ligated with double-stranded oligodeoxynucleotide I,

```
CAAGGAGATTAATTTGCAGCTGAGCCAGGAGG
   CTCTAATTAAACGTCGACTCGGTC,
```

to yield G131D154G.

Predisulfide chimera 2 (Fig. 3A, second row). G131D156G was digested with *Eag* I and *Bst*EII to yield an 800-bp fragment, which was digested with *Ava* I to yield a 570-bp *Ava* I–*Bst*EII δ–γ fragment. Ligation of the 570-bp *Ava* I–*Bst*EII fragment to the 3900-bp *Bst*EII–*Spe* I γ fragment, followed by digestion with *Spe* I, yielded the 4470-bp *Ava* I–*Spe* I δ–γ fragment, which was ligated to the 1050-bp *Spe* I–*Tth*111I γ fragment and oligonucleotide II,

```
GTGTCTTCGAGGTGGCTCTCTACTGCAATGTACTAGTGTCCCCC
 ACAGAAGCTCCACCGAGAGATGACGTTACATGATCACAGGGGGAGCC,
```

to yield predisulfide chimera 2.

Predisulfide chimera 3 (Fig. 3A, third row). Gamma-pRBG4 was digested with *Eag* I and *Bst*EII, and the 4900-bp and 790-bp fragments were isolated. The 790-bp fragment was digested with *Hph* I to yield a 480-bp fragment, which was ligated to the 4900-bp fragment and, after digestion with *Eag* I, yielded the 5380-bp *Hph* I–*Eag* I γ fragment. Predisulfide chimera 2 was digested with *Eag* I and *Spe* I to yield a 240-bp fragment, which was ligated with the 5380-bp *Hph* I–*Eag* I γ fragment and oligonucleotide III,

```
CTAGTGTCCCCCGACGGTTGTGTGACCTGGC–
                        TGCCGCCTGCCATCTTCAGATCTTCCTGCCCC
   ACAGGGGGCTGCCAACACACTGGACCG–
                        ACGGCGGACGGTAGAAGTCTAGAAGGACGGG
```

to yield predisulfide chimera 3.

Predisulfide chimera 4 (Fig. 3A, fourth row). Predisulfide chimera 3 was digested with *Bgl* II and *Bst*EII to yield a 4940-bp *Bst*EII–*Bgl* II fragment, which was ligated to the 480-bp *Hph* I–*Bst*EII γ fragment and oligonucleotide IV,

```
GATCCTCCTGCAGC
   GAGGACGTC,
```

to yield predisulfide chimera 4.

Postdisulfide chimeras (Fig. 3B). These were constructed as described for G131D156G in Fig. 2, by changing the oligonucleotide cassette (I) as needed.

Postdisulfide chimeras (Fig. 3C). G175D225G was digested with *Pfl*MI and *Bst*XI to yield a 5503-bp *Pfl*MI–*Bst*XI fragment, which was ligated to oligonucleotide V,

```
ATGGGAACAACAGATCTTACCCCATTGA
CTCCTACCCTTGTTGTCTAGAATGGGGTA,
```

to yield postdisulfide chimera 1 (see Fig. 3*C*, second row). Additional postdisulfide chimeras was prepared by changing the oligonucleotide cassette (V) as needed.

γ predisulfide point mutants. These were constructed as described for predisulfide chimera 2, by changing the oligonucleotide cassette (II) as needed.

G(S161K). Gamma-pRBG4 was digested with *Pfl*MI and *Eag* I to yield a 430-bp fragment, which was digested with *Sau*3A1 to yield a 390-bp *Eag* I–*Sau*3A1 γ fragment. Ligation of the 390-bp fragment, the 5098-bp *Bst*XI–*Eag* I γ fragment, and oligonucleotide VI,

```
GATCAACTTGCAACTCAAGCAGGAGG
   TTGAACGTTGAGTTCGTC,
```

yielded G(S161K).

δ predisulfide point mutants. Delta-pRBG4 was digested with *Eag* I and *Pfl*MI to yield a 5078-bp *Pfl*MI–*Eag* I δ fragment plus a 355-bp *Pfl*MI fragment. The 355-bp *Pfl*MI fragment was digested with *Hph* I to yield the 130-bp *Hph* I–*Pfl*MI δ fragment. Delta-pRBG4 was digested with *Eag* I and *Kpn* I to yield a 635-bp fragment, which was digested with *Ava* I to yield a 275-bp *Eag* I–*Ava* I δ fragment. The 275-bp fragment was ligated to the 5078-bp *Pfl*MI–*Eag* I δ fragment to yield the 5353-bp *Ava* I–*Pfl*MI δ fragment, which was ligated with the 130-bp *Hph* I–*Pfl*MI fragment and oligonucleotide VII,

```
TCGGGCTACGTATACTGGCTGCCGCCCGCAATATTCAGATCTTCCTGCCCC
   CGATGCATATGACCGACGGCGGGCGTTATAAGTCTAGAAGGACGGG,
```

to yield D(T118Y). Additional δ predisulfide point mutants were made by changing the oligonucleotide cassette (VII) as needed.

D(K163S). Delta-pRBG4 was digested with *Pfl*MI and *Eag* I to yield a 5078-bp *Pfl*MI–*Eag* I δ fragment. Delta-pRBG4 was digested with *Eag* I and *Sty* I to yield the 396-bp fragment, which was ligated with the 5078-bp *Pfl*MI–*Eag* I δ fragment and oligonucleotide VIII,

```
CAAGGAGATCACACTTAGTTTAAGCCAG–
                        GAGGAGGAAAACAACAGATCTTACCCCATTGA
   CTCTAGTGTGAATCAAATTCGGTCCTCCTCCTTTTGTTG–
                        TCTAGAATGGGGTA,
```

to yield D(K163S).

AChR Expression in Human Embryonic Kidney 293 Cells. AChR subunit cDNAs in the pRBG4 expression vector were transfected into HEK 293 cells (ATCC CRL 1573) by calcium phosphate precipitation. In all experiments, cDNAs were cotransfected in the following amounts per 10-cm plate of cells: α (21 μg), β (11 μg), and either γ, δ, or mutant subunits (21 μg). Cells were maintained for 3 days at 31°C in Dulbecco's modified Eagle's medium plus 10% fetal bovine serum (5). Amounts of AChR expressed in this transient system were similar to those expressed in stable cell lines; αβγ AChRs in 293 cells yielded 4–8 fmol of surface toxin binding sites per cm^2 of confluent cells, compared with 10–15 fmol/cm^2 expressed by 3T3 cells stably expressing αβγ AChRs (5).

DMT Binding Measurements. Three days after transfection, intact cells were harvested by gentle agitation in phosphate-buffered saline plus 5 mM EDTA, briefly centrifuged, suspended in high-potassium Ringer's solution (3), and divided into aliquots for DMT binding measurements. DMT binding to intact cells was measured by competition against the initial rate of binding of ^{125}I-labeled α-bungarotoxin (3). DMT was chosen for study, rather than *d*-tubocurarine, because it is about 2-fold more selective for the two binding sites, and it allows comparison with previous studies (3, 5). Fitting the Hill equation to the competition data yielded apparent dissociation constants, K_d, and Hill coefficients, n_H (3).

RESULTS

Native and mutant AChR subunit cDNAs were transiently expressed in HEK 293 fibroblasts, and DMT binding was measured by competition against α-bungarotoxin binding. The first chimera, D225G, contained δ sequence from the N terminus of the subunit to the start of the first membrane-spanning region, M1, followed by γ sequence to the C terminus. Coexpression of D225G with α and β subunits yielded high-affinity α-bungarotoxin binding sites, similar in quantity to that produced by α, β, and γ subunits. Expression of α and β subunits alone did not produce surface toxin binding sites, as first shown by Blount and Merlie (6), so any surface AChRs must contain the chimeric subunit. AChRs containing D225G showed pure δ-like binding, demonstrating that the binding determinants lie within the major extra cellular portion of the subunit (Figs. 1 and 2).

Two more chimeras, G100D225G and G175D225G, produced pure δ- and pure γ-like binding, respectively (Fig. 2), narrowing the region containing binding determinants to between residues 100 and 175 (δ-subunit numbering). Placing the γ–δ junction near the middle of this 75-residue region, as in

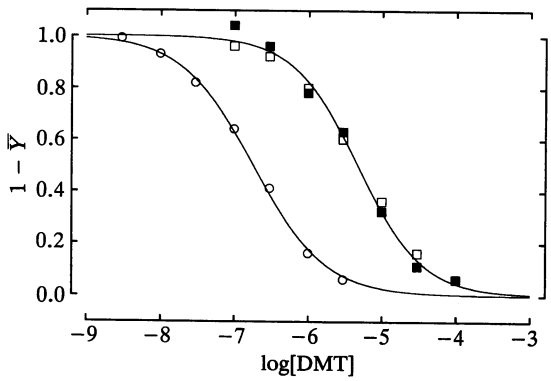

FIG. 1. Concentration dependence of DMT binding to surface AChRs composed of α, β, and γ (○); α, β, and δ (□); or α, β, and D225G (■) subunits. DMT binding is plotted as $(1 - \bar{Y})$, the rate of toxin binding in the presence of DMT divided by the rate in its absence (3). The curves through the data are fits to the Hill equation (3) with the following parameters: $\alpha\beta\gamma$, $K_d = 1.8 \times 10^{-7}$ M, $n_H = 0.9$; $\alpha\beta\delta$, $K_d = 4.9 \times 10^{-6}$ M, $n_H = 0.9$; $\alpha\beta$(D225G), $K_d = 4.7 \times 10^{-6}$ M, $n_H = 1.0$.

chimera G131D225G, produced a surprising but interesting binding profile. Affinity was intermediate between that of γ and δ, showing that the binding determinants cannot reside in a single residue but must involve two or more residues. These results place binding determinants in the vicinity of a disulfide loop, a motif found throughout the ligand-gated channel superfamily (10). Neglecting the serine/proline mismatch within the loop, two sets of binding determinants can be defined: predisulfide and postdisulfide (Fig. 2). A final chimera, G131D156G, contained γ sequences everywhere except for 25 δ residues in the center of this 75-residue region. The resulting construct produced pure γ-like binding, excluding this 25-residue portion from either set of binding determinants.

To identify binding determinants within the predisulfide domain, the γ–δ junction in G131D156G was expanded 17 residues from the beginning of the disulfide loop toward the N terminus (Fig. 3*A*, second row). The resulting construct produced intermediate affinity, as was seen in the original chimera bisecting this region (G131D225G). Intermediate affinity was observed, rather than pure δ affinity, because the postdisulfide residues were still γ. The predisulfide binding determinants are therefore likely to be within this 17-residue segment. Two more chimeras narrowed the predisulfide determinants to two residues, a valine–threonine pair in δ and an isoleucine–tyrosine pair in γ (Fig. 3*A*).

To identify postdisulfide determinants, the δ–γ junction in G131D156G was stepped one residue at a time toward the C terminus (Fig. 3*B*). The series of constructs produced high-affinity γ-like binding until serine-161 in γ was replaced by its δ homologue, lysine-163, where intermediate affinity was observed, again similar in magnitude to that seen in the initial chimeras. The postdisulfide binding determinant therefore appears to be a single residue, serine-161 in γ and lysine-163 in δ.

To look further for postdisulfide determinants, δ sequence was added in an N-terminal direction to G175D225G (Fig. 3*C*), which produced pure γ-like binding in Fig. 2. The first construct added the four δ residues missing in all γ subunits; among these four residues is a conserved arginine/lysine which might be expected to produce low affinity for a positively charged ligand such as DMT. The binding curve nevertheless showed high-affinity γ-like binding. The second construct introduced the trio of consecutive glutamate residues found in δ, but still produced pure γ-like binding. These results strongly suggest that only one residue in the postdisulfide region affects DMT affinity, serine-161 in γ and lysine-163 in δ.

The preceding results identify three residues in the γ and δ subunits likely to determine DMT selectivity. To confirm these assignments, point mutations were introduced into the three key positions of both subunits (Fig. 4). For this discussion, mutants are designated according to the residues present at the three key positions I, II, and III, and mutant residues are underlined; pure γ, for example, is G(IYS). In the γ subunit, mutating a single residue to the corresponding δ residue affected DMT affinity quantitatively, in line with affinity changes seen in the above described chimeras. The tyrosine → threonine switch [G(I<u>T</u>S)] produced the greatest decrease in affinity, followed by a smaller decrease produced by the serine → lysine switch [G(IY<u>K</u>)], and finally a barely detectable change with the isoleucine → valine switch [G(<u>V</u>YS)]. Combining mutations at the pre- and postdisulfide positions produced roughly additive changes in binding af-

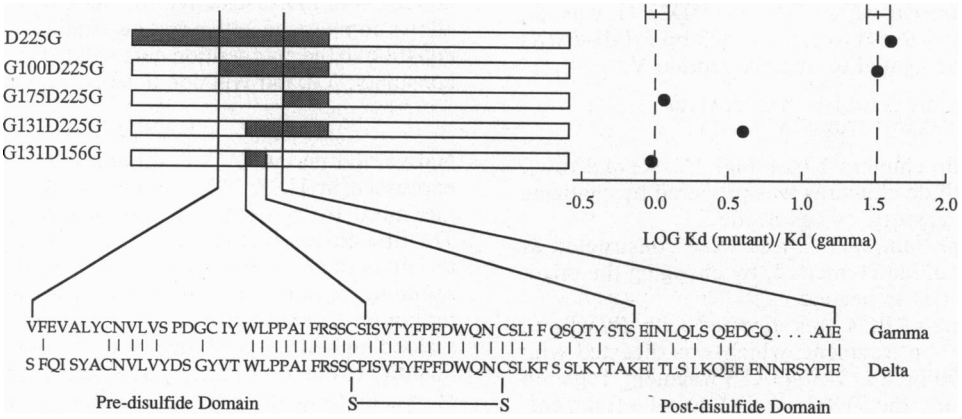

FIG. 2. DMT binding affinity of δ–γ subunit chimeras. (*Upper Left*) Schematic drawings of the subunit chimeras. Shading represents δ sequences, and unshaded portions represent γ sequences; regions of sequence identity are not shown. Chimeras are designated as described under *Methods*. (*Upper Right*) DMT binding affinity for the five chimeras, plotted as the ratio of the K_d of AChRs containing the mutant subunit to the K_d of AChRs containing the γ subunit. The K_d was determined by fitting the Hill equation to each set of binding data, as in Fig. 1. Hill coefficients are not presented, but were all close to 1.0, except for G131D225G, for which $n_H = 0.8$. For each chimera, DMT binding was measured for both γ- and δ-containing triplet AChRs in the same experiment. Dashed lines show mean K_d ratios for triplet AChRs containing either γ or δ subunits, and bars give standard deviations for γ- or δ-containing AChRs measured in these five experiments. In all experiments DMT binding to surface AChRs was measured as described under *Methods*. (*Lower*) Residues containing binding determinants. The γ and δ sequences are aligned, with identical residues marked by vertical lines. Predisulfide determinants are between residues 100 and 131, shown by the left set of vertical bars. Postdisulfide determinants are between residues 157 and 175, shown by the right set of vertical bars.

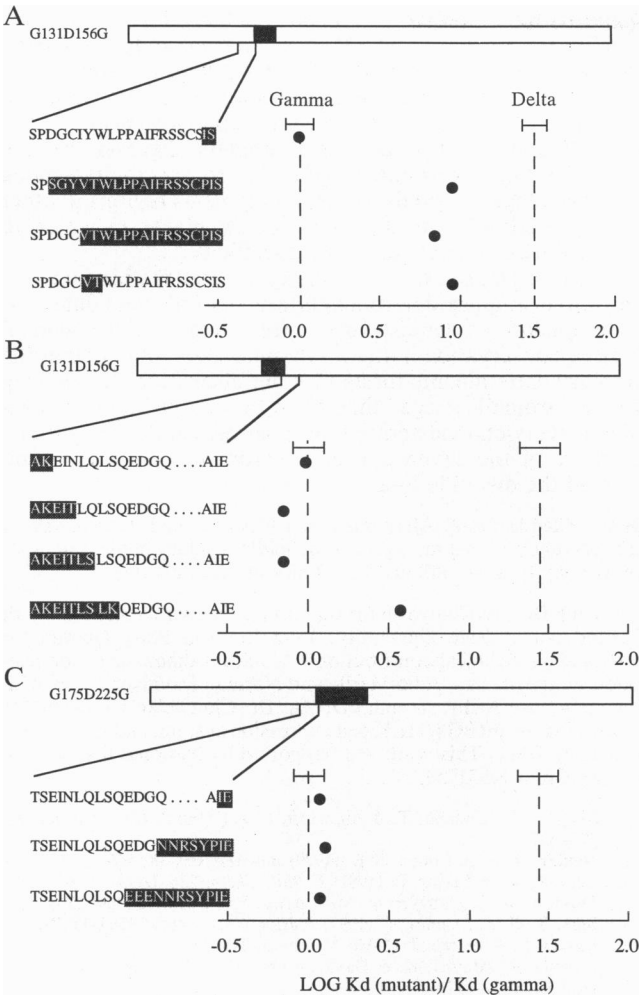

FIG. 3. (*A*) Determination of DMT binding determinants in the predisulfide region. The sequence in the first row is G131D156G from Fig. 2, where it showed pure γ-like binding. K_d values for DMT were determined as in Figs. 1 and 2; the fitted Hill coefficients were not significantly different from 1.0. This series of constructs shows that the predisulfide determinant contains one or both of two homologous residues, VT in δ and IY in γ. (*B*) Determination of DMT binding determinants in the postdisulfide region. The sequence in the first row is G131D156G from *A*, where it showed pure γ-like binding. High-affinity γ-like binding is seen until serine-161 in γ is replaced by its δ homologue, lysine-163, where intermediate binding affinity is seen. (*C*) Further examination of postdisulfide determinants. The sequence in the first row is G175D225G from Fig. 2, where it showed pure γ-like binding. Pure γ-like binding is seen throughout, excluding these δ sequences from the set of binding determinants.

finity, as can be seen by comparing G(IYK) with G(ITK), for example. G(ITK) decreased binding affinity beyond that of pure delta [D(VTK)]. However, simultaneous mutation of all three residues to their δ counterparts, as in G(VTK), quantitatively reconstructed the pure δ binding curve.

Introducing the three key γ residues into the δ subunit, singly or in combination, produced changes in DMT binding affinity roughly equal in magnitude but opposite in direction to those produced in the γ subunit. Most important, pure high-affinity γ-like binding was produced in the δ subunit by simultaneous mutation of the three above identified residues (Fig. 4). In the δ subunit, however, quantitative changes in affinity were observed which provide insight into how the valine–isoleucine determinant affects DMT binding. First, pure γ-like binding was observed in the single residue mutant D(VYK); in the absence of information about the other two key residues, the threonine → tyrosine mutation alone would

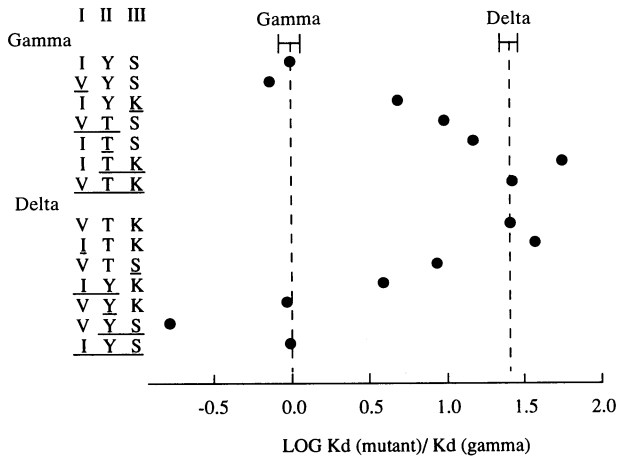

FIG. 4. Point mutations in the γ and δ subunits. The indicated point mutations were introduced into the γ and δ subunits, and K_d values for DMT were determined as in Figs. 1–3; for all point mutants, the fitted Hill coefficients were not significantly different from 1.0. Vertical dashed lines show the mean affinity ratios for γ- and δ-containing triplet AChRs, and bars show standard deviations for this set of 12 experiments. Simultaneous mutation of the three binding determinants produced γ-like binding in the δ subunit and produced δ-like binding in the γ subunit.

appear to account for the difference between δ and γ binding affinity. However, introducing the valine → isoleucine mutation into D(VYK), as in D(IYK), decreased binding affinity by a factor of about 3 relative to that of D(VYK), much greater than the barely detectable change produced by the valine → isoleucine mutation alone [D(ITK)]. A similar nonlinear contribution can be seen by comparing the double mutant D(VYS) with the triple mutant D(IYS); the difference between the double and triple mutants is again much greater than that produced by the valine → isoleucine mutation alone. Thus when δ has tyrosine at determinant position II, addition of one methyl group to the neighboring residue, as in D(IYK) and D(IYS), strongly decreases binding affinity; the additional methyl group may sterically displace the phenol side chain into a position less favorable for docking with DMT.

DISCUSSION

These experiments identify residues in the γ and δ subunits that give the two binding sites in the AChR different affinity for curariform antagonists. Although it is tempting to conclude that these residues actually form part of the binding pocket, one cannot exclude an allosteric affect on the pocket. Electrostatic considerations, however, favor a direct shaping mechanism; the quaternary nitrogens in DMT would associate more tightly with tyrosine and serine in γ than with threonine and lysine in δ, in line with the measured subunit affinities. Also, the free energy of binding contributed by the pre- and postdisulfide determinants is roughly additive, as would be expected in a shaping mechanism but might not be expected in an allosteric one. Systematically varying residues at each position may shed further light on mechanism.

These results also suggest that the γ and δ subunits contribute very similar basic scaffolds to the binding pocket and that the pre- and postdisulfide residues occupy equivalent positions within the γ and δ scaffolds. Considering a rigid ligand such as DMT, one would not expect the observed linear and interchangeable alterations in affinity if the pre- and postdisulfide determinants were not held in nearly the same positions at both the α–γ and α–δ subunit interfaces.

While the pre- and postdisulfide residues determine selectivity of curare for the two binding sites, it is likely that other parts of the AChR further stabilize curare within each site. Photoaffinity labeling with *d*-tubocurarine reveals labeling of

homologous tryptophans in the γ (W55) and δ (W57) subunits (11); these residues do not affect selectivity, but may provide additional stabilizing interactions. Mutagenesis of residues in the α subunit also affects curare affinity (unpublished observations and ref. 12), providing yet another possible source of stabilizing interactions. Combining results from mutagenesis studies with recent high-resolution images of the putative binding pocket suggests the following picture of the curare-binding domain. The ligand-binding pocket appears to be a gorge centered within the α subunit (13), but with one wall formed by the adjacent non-α subunit, presumably γ or δ. The two quaternary nitrogens of curare are 10.8 Å apart, a distance that would allow it to bridge from the center of the α portion of the binding pocket to the neighboring γ or δ subunit.

Structurally conspicuous is the disulfide loop bounded by the pre- and postdisulfide binding determinants. Containing 13 highly conserved residues between the two cysteines (Fig. 2), this loop is found in all acetylcholine, γ-aminobutyrate, glycine, and type 3 serotonin receptor subunits (10). Also conspicuous is the high degree of sequence identity in the 10 residues preceding the loop and the four residues following it (Fig. 2). Such strong conservation in this region supports the close structural similarity between the γ and δ subunits inferred from the present binding experiments. The functional significance of this loop must remain speculative, but its ubiquity among ligand-gated channel subunits and its proximity to the DMT binding determinants suggest roles either in contributing to the ligand-binding pocket or in coupling agonist binding to channel functions, such as opening or desensitization.

For the γ subunit, the three binding determinants are well conserved among species for which these subunits have been sequenced [mouse (7, 8), rat (14), calf (15, 16), chicken (17), *Xenopus* (18), *Torpedo* (19, 20), and human (21, 22)]. Determinant II is tyrosine in all species, determinant III is serine or threonine, and determinant I is isoleucine, valine, or methionine (Fig. 5). Looking beyond the muscle AChR, one finds that certain γ-aminobutyrate (23) and glycine (24) receptor subunits contain tyrosine in a position homologous to determinant II in γ. This predisulfide tyrosine may therefore represent a binding-site signature in these non-AChR subunits.

Among δ subunits, the three binding determinants are not well conserved across species (Fig. 5). Determinant III is partially conserved, being arginine or lysine in all species except *Torpedo*, which has methionine. The most notable deviation is determinant II, a threonine in mouse, but tyrosine in calf, chicken, frog, and human. In species containing tyrosine at position II, γ and δ would differ only at positions

Gamma	Predisulfide	Postdisulfide
	I II	III
Mouse	DGCIYWLPP	LQLSQED
Rat	DGCIYWLPP	LQLSQED
Calf	DGCVYWLPP	LQLSQED
Chick	DGSIYWLPP	LLLTVEE
Frog	DGSMYWLPP	LLLTVDE
Torpedo	DGSMYWLPP	LQLSAEE
Human	DGCIYWLPP	LQLSQED

Delta	Predisulfide	Postdisulfide
	I II	III
Mouse	SGYVTWLPP	LSLKQEE
Rat	SGHVTWLPP	LSLKQEE
Calf	SGSVYWLPP	LSLKQAE
Chick	TGYVYWLPP	MHLKEES
Frog	DGFMYWLPP	LQLRQDL
Torpedo	NGYVTWLPP	MDLMTDT
Human	YGFVYWLPP	LSLKNDA

FIG. 5. Sequence alignment of segments containing the pre- and postdisulfide binding determinants for the γ and δ subunits. Binding determinant residues are labeled I–III as in Fig. 4.

I and III, thus predicting a much smaller difference in DMT affinity for the two sites. Of these species, only the human AChR has been examined for DMT binding; it shows only a 3-fold difference in the binding affinities of the two sites (25), in contrast to the nearly 100-fold difference seen in mouse (9). The general variation among δ subunits suggests that the three binding determinants give rise to specificity among pharmacological ligands. Thus, homologous regions in other ligand-gated subunits represent logical places in which to look for determinants of ligand specificity.

Because DMT competes with agonist for the binding site, the three binding determinants are natural candidates for determinants of agonist specificity. However, the general lack of conservation in the δ subunit makes it likely that the primary determinants for agonist are elsewhere. By analogy to the "aromatic gorge" that forms the acetylcholine binding site in acetylcholinesterase (26), possible candidates are one or more of the seven conserved aromatic residues in and around the disulfide loop.

Note Added in Proof. After this paper was accepted, Czajkowski *et al.* (27) reported that mutagenesis of acidic residues in the δ subunit, most notably D180, affects the affinity of acetylcholine.

I thank Dr. Fred Sigworth for support and encouragement for work carried out at Yale University, Ling Lin and Polly Quiram for outstanding technical contributions, Monica Talmor for oligonucleotide synthesis, Drs. John Merlie and Norman Davidson for providing the mouse AChR subunit cDNAs, Dr. Chinweike Ukomadu for suggesting the pRBG4/HEK cell expression system, and Eli Lilly for providing DMT. This work was supported by National Institutes of Health Grant NS31744.

1. Sine, S. M., Claudio, T. & Sigworth, F. J. (1990) *J. Gen. Physiol.* **96,** 395–437.
2. Neubig, R. R. & Cohen, J. B. (1979) *Biochemistry* **18,** 5464–5475.
3. Sine, S. M. & Taylor, P. (1981) *J. Biol. Chem.* **256,** 6692–6699.
4. Jackson, M. B. (1989) *Proc. Natl. Acad. Sci. USA* **86,** 2199–2203.
5. Sine, S. M. & Claudio, T. (1991) *J. Biol. Chem.* **266,** 19369–19377.
6. Blount, P. & Merlie, J. (1990) *Neuron* **3,** 349–357.
7. LaPolla, R., Mayne, K. & Davidson, N. (1984) *Proc. Natl. Acad. Sci. USA* **81,** 7970–7974.
8. Yu, L., LaPolla, R. & Davidson, N. (1986) *Nucleic Acids Res.* **14,** 3539–3555.
9. Lee, B. S., Gunn, R. B. & Kopito, R. R. (1991) *J. Biol. Chem.* **266,** 11448–11456.
10. Betz, H. (1990) *Neuron* **5,** 383–391.
11. Chiara, D. C. & Cohen, J. B. (1992) *Biophys. J.* **61,** A106 (abstr.).
12. O'Leary, M. E. & White, M. M. (1992) *Soc. Neurosci. Abstr.* **18,** 259.1.
13. Unwin, N. (1993) *J. Mol. Biol.* **229,** 1101–1124.
14. Witzemann, V., Stein, E., Barg, B., Konno, T., Koenen, M., Kues, W., Criado, M., Hofmann, M. & Sakmann, B. (1990) *Eur. J. Biochem.* **194,** 437–448.
15. Takai, T., Noda, M., Furutani, Y., Takahashi, H., Notake, M., Shimizu, S., Kayano, T., Tanabe, T., Tanaka, K., Hirose, T., Inayama, S. & Numa, S. (1984) *Eur. J. Biochem.* **143,** 109–115.
16. Kubo, T., Noda, M., Takai, T., Tanabe, T., Kayano, T., Shimizu, S., Tanaka, K., Takahashi, H., Hirose, T., Inayama, S., Kikuno, R., Miyata, T. & Numa, S. (1985) *Eur. J. Biochem.* **149,** 5–13.
17. Nef, P., Mauron, A., Stalder, R., Alliod, C. & Ballivet, M. (1984) *Proc. Natl. Acad. Sci. USA* **81,** 7975–7979.
18. Baldwin, T., Yoshihara, C., Blackmer, K., Kintner, C. & Burden, S. (1988) *J. Cell Biol.* **106,** 469–478.
19. Noda, M., Furutani, Y., Takahashi, H., Toyosato, M., Tanabe, T., Shimizu, S., Kikyotani, S., Kayano, T., Hirose, T., Inayama, S. & Numa, S. (1983) *Nature (London)* **302,** 528–532.
20. Claudio, T., Ballivet, M., Patrick, J. & Heinemann, S. (1983) *Proc. Natl. Acad. Sci. USA* **80,** 1111–1115.
21. Shibahara, S., Kubo, T., Perski, H., Takahashi, H., Noda, M. & Numa, S. (1985) *Eur. J. Biochem.* **146,** 15–22.
22. Luther, M., Schoepfer, R., Whiting, P., Casey, B., Blatt, Y., Montal, M. S., Montal, M. & Lindstrom, J. (1989) *J. Neurosci.* **9,** 1082–1096.
23. Shivers, B. D., Killisch, I., Sprengel, R., Sontheimer, H., Kohler, M., Schofield, P. & Seeburg, P. (1989) *Neuron* **3,** 327–337.
24. Grenningloh, G., Rienitz, A., Schmitt, B., Methfessel, C., Zensen, M., Beyreuther, K., Gundelfinger, E. & Betz, H. (1987) *Nature (London)* **328,** 215–220.
25. Sine, S. M. (1988) *J. Biol. Chem.* **263,** 18052–18062.
26. Sussman, J. L., Harel, M., Frolow, F., Oefner, C., Goldman, A., Token, L. & Silman, I. (1991) *Science* **253,** 872–879.
27. Czajkowski, C., Kaufmann, C. & Karlin, A. (1993) *Proc. Natl. Acad. Sci. USA* **90,** 6285–6289.